Available online at www.sciencedirect.com

ScienceDirect

Mendeleev Commun., 2024, **34**, 847–849

Mendeleev Communications

Silicate-substituted hydroxyapatite bioceramics fabrication from the amorphous powder precursor obtained from the silicate-containing solutions

Daniil O. Golubchikov,*[a,b] Tatiana V. Safronova,[a,c] Vladimir A. Podlyagin,[a] Tatiana B. Shatalova,[a,c] Irina V. Kolesnik[a,c] and Valery I. Putlayev[a,c]

[a] *Department of Materials Science, M. V. Lomonosov Moscow State University, 119991 Moscow, Russian Federation. E-mail: golubchikovdo@my.msu.ru*

[b] *Institute for Regenerative Medicine, I. M. Sechenov First Moscow State Medical University, 119991 Moscow, Russian Federation*

[c] *Department of Chemistry, M. V. Lomonosov Moscow State University, 119991 Moscow, Russian Federation*

DOI: 10.1016/j.mencom.2024.10.025

The mixed-anionic solution synthesis was applied to obtain X-ray amorphous powder precursor of silicon-substituted hydroxyapatite (Si-HAp) for macroporous bioceramics fabrication. Proposed technique was proven to provide small particle size up to 1 μm, as well as homogeneous components distribution in the final Si-HAp ceramics. A possible pathway of the Si-HAp formation under gradual heating up to 1000 °C was discussed.

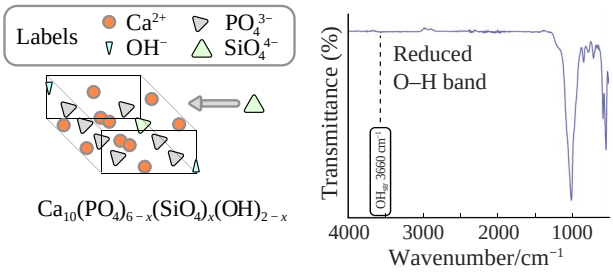

Keywords: bone tissue engineering, bioceramics, mixed-anionic solution, amorphous calcium phosphate, calcium silicate, hydroxyapatite, silicate-substituted hydroxyapatite.

Bone tissue restoration remains challenging, especially for healing large bone defects.[1–4] However, conventionally employed calcium phosphates do not provide relevant degradation rate, thereby, modern studies aim at producing more soluble materials.[5–7] In particular, bioceramics based on calcium phosphates/silicates were considered as promising compositions for bone tissue repair.[8] The presented system appears as a part of the Na_2O–CaO–SiO_2–P_2O_5, pioneered by Hench *et al.*[9,10] Further studies authenticated the positive effect of the silicate substitution on the *in vitro* bioceramics resorption rate in comparison with non-substituted β-tricalcium phosphate (β-TCP),[11–13] inasmuch as Si-rich layers provide sites for the hydroxyapatite (HAp) formation.[13] Moreover, silicate-based bioceramics were found to enhance osteogenic differentiation in comparison with β-TCP and HAp materials, that was proven by higher alkaline phosphatase (ALP) activity and bone morphogenetic protein (BMP-2) content.[14–16] In addition, silicate insertion in the HAp lattice results in the increased solubility, in particular, silicate-substituted hydroxyapatite (Si-HAp) has shown the extensive dissolution in simulated body fluid (SBF) after 3 days.[17]

Earlier, a number of approaches to obtain substituted calcium phosphates have been reported. Some of the powder precursors were prepared mechanochemically,[18,19] however, precipitation from the mixed-anionic solutions has proven to be an effective way of obtaining mixed phases from the HPO_4^{2-}/CO_3^{2-}, SiO_3^{2-}/PO_4^{3-} and SO_4^{2-}/PO_4^{3-} solutions.[20–22] Moreover, the selected path allowed one to achieve a highly uniform component distribution over ceramics bulk and small precursor particles formation, which was considered as an essential parameter for macroporous implants fabrication by stereolithographic 3D printing.

Solution-based synthesis remains the most available and widely used way to produce ceramics powder precursors.[21] However, sodium by-products adsorbed from the solution on the precipitate surface may act as a sintering additive causing the Na-containing phases formation at 800 °C.[21,23] Thereby, sodium

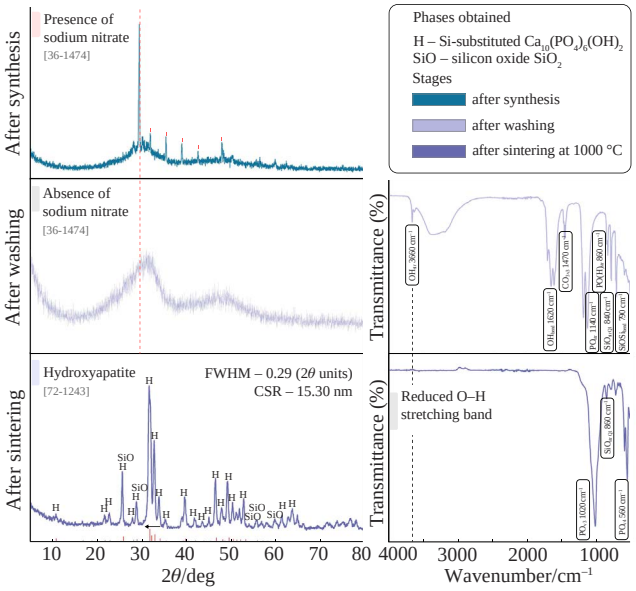

Figure 1 XRD and FTIR spectra for powders after synthesis, washing and ceramics after sintering at 1000 °C.

salts should be removed from the powder precursor before the ceramics manufacturing.[24,25]

In this work, we propose the novel way to produce powder precursor with small particle size and uniform components distribution for the fabrication of ceramics based on silicate-substituted HAp *via* the mixed-anionic synthesis. Another benefit of this technique over the conventional synthesis from silicon orthoesters is the silicate anion presence in the amorphous powder precursor. Otherwise, silicon is present in the form of hydrated silica, that requires long-term heat treatment to ensure silicon introduction into the HAp lattice.[26]

The powder synthesis was carried out using the amounts of Na_2SiO_3, $Ca(NO_3)_2$ and Na_2HPO_4 calculated according to the following equation:†

$$2Ca(NO_3)_2 + Na_2HPO_4 + Na_2SiO_3 + xH_2O \rightarrow CaHPO_4{\cdot}2H_2O + CaSiO_3{\cdot}xH_2O + 4NaNO_3 \quad (1)$$

The powder XRD analysis after washing revealed the absence of sodium nitrate in the composition (see Figure 1).

It is worth to note, that washing process has resulted in the partial crystallization of powders, inasmuch as the initial composition of samples after synthesis has been represented by X-ray amorphous phase, probably, amorphous calcium phosphate (ACP) and calcium silicate hydrate, which have been recently obtained in the same conditions.[21,27] Silicate phase formation was confirmed by the Si–O stretching band (860–840 cm^{-1}) and Si–O–Si band (790 cm^{-1}) at the corresponding IR spectra. According to the SEM images, highly porous powders with the submicron particle size were obtained after the synthesis/washing (Figure 2). Further gradual heating yielded the ACP crystallization into non-stoichiometric HAp. The significant benefit of the mixed-anionic synthesis, implemented in the presented study, was obtaining the smaller particles than previously reported for other techniques.[28] Moreover, the uniform components distribution, including silicon and phosphorous, was revealed by EDX-mapping analysis, that was also declared as a mixed-anionic approach benefit (for details, see Online Supplementary Materials).

According to the thermogravimetric data (TG), the final mass loss of the powder after heating up to 1000 °C was 18%. The first stage exhibited at the TG curve was associated with the gradual water elimination up to 200 °C. Two DTA peaks at 80 and 200 °C could be attributed to the removal of physisorbed water and chemically bonded water, respectively.[29] Highly charged silicate anions were previously reported to retain water in the apatite structure at higher temperatures up to 600 °C, but this effect was hardly observed in the current study, due to the massive water elimination below 200 °C. DTA peaks at 800 and 850 °C could be related to the process of carbonates decomposition, presence of which was proven by the IR spectra.

† Powder precursor was synthesized from the water solution of calcium nitrate (ACS reagent, Sigma-Aldrich, Mumbai, India) and mixed-anionic solution, which simultaneously contained sodium metasilicate (RusKhim, Moscow, Russia) and sodium phosphate dibasic (BioXtra, Sigma-Aldrich, Gillingham, UK). The starting salts were dissolved in distilled water at the concentration of 0.5 M, then the calcium salt solution was slowly added to the sodium salts solution in the volume ratios corresponding to the reaction (1), and the suspension was stirred for 1 h. The synthesis was carried out at 37 °C. Then, the precipitate was filtered using a vacuum filter and evenly distributed over a large surface area and left to dry for 1 week. After drying 20 g of synthesized powder were placed in 200 ml of distilled water. The procedure of washing and the collection of washing liquid was repeated 4 times. Powder washing was aimed at removing the reaction by-products ($NaNO_3$) which could act as a sintering additive and induce the multiphase composites formation.

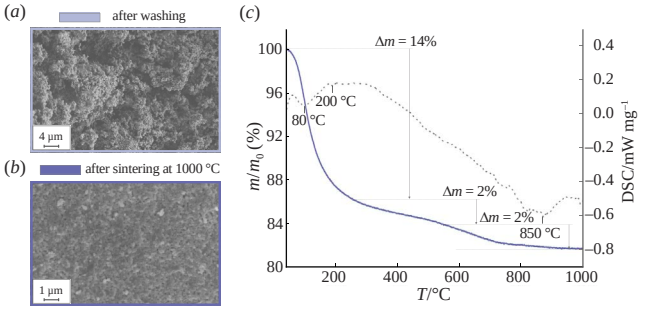

Figure 2 SEM images of powder after (*a*) synthesis and washing, (*b*) sintering at 1000 °C and (*c*) thermogravimetry and differential thermal analysis curves.

Further sintering of the compacted powder samples at 1000 °C was carried out in order to study the effect of high temperatures on the initial composition and to obtain bioceramics based on Si-substituted HAp.‡ Si-substituted hydroxyapatite formed by the reaction (2) at 1000 °C:

$$(6-x)/6Ca_{10}(PO_4)_6(OH)_2 + (5/3)xCaSiO_3{\cdot}nH_2O \rightarrow Ca_{10}(PO_4)_{6-x}(SiO_4)_x(OH)_{2-x} + [(1/3)x + n]H_2O + (2/3)xSiO_2 \quad (2)$$

The reaction equation (2) is relevant to stoichiometric HAp. Whereas silicate-ions were not expected to be introduced to the HAp lattice after the synthesis, non-stoichiometric HAp was more likely to precipitate *de facto*,[30] so less SiO_2 was observed in the final powder composition. Thereby, reaction equation (2) can be modified in accordance with the Ca- and OH-deficient HAp formation. O–H band at 3660 cm^{-1} was not observed for sintered powders, while this band was presented in the spectrum of washed sample. Thereby, it is possible to prove the partial OH substitution in the hydroxyapatite structure according to the following scheme:

$$PO_4^{3-}{}_{PO_4} + OH^-{}_{OH} \leftrightarrow SiO_4^{4-}{}_{PO_4} + V_{OH} \quad (3)$$

Moreover, IR spectra of the sintered samples included Si–O stretching (860–840 cm^{-1}) and Si–O–Si (790 cm^{-1}) bands accompanied by the broad hydroxyapatite bands (1100–1000 cm^{-1} and 560 cm^{-1}), which demonstrated the presence of silicate

‡ To produce ceramics in a form of pellets, powder was pressed into the form of simple disks by uniaxial one-sided pressing on a manual press (Carver Laboratory Press Model C, Fred S. Carver, Inc., Wabash, IN, USA) using steel die with a diameter of 12 mm at the pressure of 100 MPa for 10 s. The powder samples in a form of discs were sintered at 1000 °C to control the phase transformations and microstructure formation. Heating in the furnace was carried out at heating rate of 5 °C min^{-1}. The holding time was 2 h. The density of the samples before and after the heat treatment was calculated using the following equation: $\rho = m/(h \times \pi D^2/4)$ g cm^{-3}, where ρ – density of the sample; m – weight of the sample; h – thickness of the sample; D – diameter of the sample. The mass and the linear dimensions of the samples were measured with accuracy of ±0.001 g and ±0.01 mm, before and after the heat treatment, respectively. Thermal analysis (TA) including thermogravimetry (TG) and differential thermal analysis (DTA) were performed using an STA 409 PC Luxx thermal analyzer (NETZSCH, Selb, Germany) during heating in air (10 °C min^{-1}, 40–1000 °C), the specimen mass being at least 10 mg. The phase composition of the powders was determined by X-ray powder diffraction (XRD) analysis using Rigaku D/Max-2500 diffractometer (Rigaku Corporation, Tokyo, Japan) with a rotating anode (CuKα radiation), angle interval 2θ from 5° to 80° (2θ step was 0.02°). Microscopic images were obtained by SEM on a LEO SUPRA 50VP FEG electron microscope (Carl Zeiss, Jena, Germany) at the accelerating voltage of 3–20 kV using an SE2-detector. IR spectra were collected using Spectrum 3 FTIR spectrometer (Perkin Elmer, Waltham, MA, USA) in ATR mode in the wavenumber range of 4000–520 cm^{-1} with Universal ATR accessory (diamond/KRS-5 crystal).

groups in the final composition. In addition to the FTIR spectroscopy data, hydroxyapatite lattice parameters may act as an additional validation of the silicate substitution. Using the Jana 2006 software, the lattice parameters were calculated on the basis of the ICDD card of hydroxyapatite ($P6_3/m$) [72-1243] (a = 9.432 Å, c = 6.881 Å, V = 530.1 Å^3). The slight decrease in a (9.426 Å) parameter was observed, while c (6.918 Å) and V (532.3 Å^3) raised, and the same trend was demonstrated for silicate-substituted HAp.[17–19] It is worth to note that the silicate introduction into the HAp lattice takes place only after sintering, according to the reaction (2), whereas the solution-based synthesis has not allowed to obtain such phases, though it still ensures silicate anion presence in the amorphous powder precursor. Moreover, previous studies revealed the occurrence of surface 'silica gel' units in HAp compositions, which can be explicated by the reaction (2).[31] After the sintering of pellets, we obtained the dense microporous ceramics (1.77 ± 0.04 g cm^{-3}). The average grain size was 200–300 nm, as silicate ions were reported to decrease grain boundary mobility.[32] It is also worth to note, that the microstructural properties of hydroxyapatite-based ceramics are largerly dependent on the sintering conditions,[24] thereby, further study to determine the optimal sintering conditions is required.

Thus, the proposed solution-based synthesis of the Si-HAp powder precursor was demonstrated to surpass the conventional approaches, reducing the precursor particle size and firing temperature necessary to obtain final ceramics. The introduction of biologically essential silicate to the HAp lattice was confirmed by reduced OH band at the IR spectra. The elements distribution uniformity was also verified. Listed factors allow for consideration the proposed technique for the macroporous bioceramics fabrication in the bone tissue engineering *via* stereolithographic 3D printing.

This work was carried out with financial support from the Russian Science Foundation (grant no. 22-19-00219) and using the equipment of the MSU Shared Research Equipment Center 'Technologies for obtaining new nanostructured materials and their complex study' and purchased by MSU in the frame of the Equipment Renovation Program (National Project 'Science'), and in the frame of the MSU Program of Development: Rigaku D/Max-2500 diffractometer, LEO SUPRA 50VP FEG scanning electron microscope, STA 409 PC Luxx thermal analyzer, Perkin Elmer PE-1600 FTIR.

Online Supplementary Materials

Supplementary data associated with this article can be found in the online version at doi: 10.1016/j.mencom.2024.10.025.

References

1 X. Huang, Y. Lou, Y. Duan, H. Liu, J. Tian, Y. Shen and X. Wei, *Bioact. Mater.*, 2024, **33**, 129; https://doi.org/10.1016/j.bioactmat.2023.10.031.
2 G. Kazakova, T. V. Safronova, D. Golubchikov O. Shevtsova and J. V. Rau, *Materials*, 2021, **14**, 4857; https://doi.org/10.3390/ma14174857.
3 D. Golubchikov, P. Evdokimov, D. Zuev, Y. Filippov, T. Shatalova and V. Putlayev, *Materials*, 2023, **16**, 3077; https://doi.org/10.3390/ma16083077.
4 S. A. Tikhonova, P. V. Evdokimov, V. I. Putlyaev, D. O. Golubchikov, A. M. Murashko, N. V. Leontiev, Ya. Yu. Filippov and I. M. Shcherbakov, *Inorg. Mater. Appl. Res.*, 2023, **14**, 349; https://doi.org/10.1134/S2075113323020466.
5 I. I. Preobrazhenskiy and V. I. Putlyaev, *Mendeleev Commun.*, 2023, **33,** 531; https://doi.org/10.1016/j.mencom.2023.06.029.
6 Y. Lukina, S. Kotov, L. Bionyshev-Abramov, N. Serejnikova, R. Chelmodeev, R. Fadeev, O. Toshev, A. Tavtorkin, M. Ryndyk, D. Smolentsev, N. Gavryushenko and S. Sivkov, *Ceramics*, 2023, **6**, 168; https://doi.org/10.3390/ceramics6010011.
7 D. M. Zuev, D. O. Golubchikov, P. V. Evdokimov and V. I. Putlyaev, *Russ. J. Inorg. Chem.*, 2022, **67**, 940; https://doi.org/10.1134/S0036023622070257.
8 J. Zhang, F. Deng, X. Liu, Y. Ge, Y. Zeng, Z. Zhai, C. Ning and H. Li, *J. Orthop. Transl.*, 2022, **32**, 103; https://doi.org/10.1016/j.jot.2021.12.002.
9 L. L. Hench, R. J. Splinter, W. C. Allen and T. K. Greenlee, *J. Biomed. Mater. Res.*, 1971, **5**, 117; https://doi.org/10.1002/jbm.820050611.
10 L. L. Hench and H. A. Paschall, *J. Biomed. Mater. Res.*, 1973, **7**, 25; https://doi.org/10.1002/jbm.820070304.
11 K. A. Hing, P. A. Revell, N. Smith and T. Buckland, *Biomaterials*, 2006, **27**, 5014; https://doi.org/10.1016/j.biomaterials.2006.05.039.
12 M. R. Kaimonov and T. V. Safronova, *Materials*, 2023, **16**, 5981; https://doi.org/10.3390/ma16175981.
13 F. Pupilli, A. Ruffini, M. Dapporto, M. Tavoni, A. Tampieri and S. Sprio, *Biomimetics*, 2022, **7**, 112; https://doi.org/10.3390/biomimetics7030112.
14 G. A. Fielding, N. Sarkar, S. Vahabzadeh and S. Bose, *J. Funct. Biomater.*, 2019, **10**, 48; https://doi.org/10.3390/jfb10040048.
15 L. Fei, C. Wang, Y. Xue, K. Lin, J. Chang and J. Sun, *J. Biomed. Mater. Res., Part B*, 2011, **100**, 1237; https://doi.org/10.1002/jbm.b.32688.
16 P. Thaitalay, O. Thongsri, R. Dangviriyakul, S. Srisuwan, L. Carney, J. E. Gough and S. T. Rattanachan, *J. Biomed. Mater. Res., Part A*, 2023, **111**, 1406; https://doi.org/10.1002/jbm.a.37542.
17 A. E. Porter, C. M. Botelho, M. A. Lopes, J. D. Santos, S. M. Best and W. Bonfield, *J. Biomed. Mater. Res., Part A*, 2004, **69**, 670; https://doi.org/10.1002/jbm.a.30035.
18 N. V. Bulina, M. V. Chaikina, I. Yu. Prosanov and D. V. Dudina, *Mater. Sci. Eng. B*, 2020, **262**, 114719; https://doi.org/10.1016/j.mseb.2020.114719.
19 N. V. Bulina, M. V. Chaikina, A. S. Andreev, O. B. Lapina, A. V. Ishchenko, I. Yu. Prosanov, K. B. Gerasimov and L. A. Solovyov, *Eur. J. Inorg. Chem.*, 2014, **28**, 4803; https://doi.org/10.1002/ejic.201402246.
20 T. V. Safronova, V. I. Putlyaev, Ya. Yu. Filippov, A. V. Knot'ko, E. S. Klimashina, K. Kh. Peranidze, P. V. Evdokimov and S. A. Vladimirova, *Glass Ceram.*, 2018, **75**, 118; https://doi.org/10.1007/s10717-018-0040-7.
21 D. Golubchikov, T. V. Safronova, E. Nemygina, T. B. Shatalova, I. N. Tikhomirova, I. V. Roslyakov, D. Khayrutdinova, V. Platonov, O. Boytsova, M. Kaimonov, D. A. Firsov and K. A. Lyssenko, *Coatings*, 2023, **13**, 374; https://doi.org/10.3390/coatings13020374.
22 L. Medvecky, M. Giretova, R. Stulajterova, L. Luptakova and T. Sopcak, *Materials*, 2021, **14**, 2137; https://doi.org/10.3390/ma14092137.
23 S. J. Kalita, S. Bose, H. L. Hosick and A. Bandyopadhyay, *Biomaterials*, 2004, **25**, 2331; https://doi.org/10.1016/j.biomaterials.2003.09.012.
24 M. Trzaskowska, V. Vivcharenko and A. Przekora, *Int. J. Mol. Sci.*, 2023, **24**, 5083; https://doi.org/10.3390/ijms24065083.
25 F. Han, L. Yu, G. Wen, J. Guo, C. Ran and S. Gu, *J. Mater. Res. Technol.*, 2022, **19**, 866; https://doi.org/10.1016/j.jmrt.2022.05.080.
26 M.-K. Mafina, R. M. Wilson, G. J. Rees, P. Gierth, A. C. Sullivan and K. A. Hing, *Acad. Mat. Sci.*, 2023, **1**, 1; https://doi.org/10.20935/AcadMatSci6121.
27 S. Chen, D. Liu, L. Fu, B. Ni, Z. Chen, J. Knaus, E. V. Sturm, B. Wang, H. J. Haugen, H. Yan, H. Cölfen and B. Li, *Adv. Mater.*, 2023, **35**, 2301422; https://doi.org/10.1002/adma.202301422.
28 A. P. Solonenko, A. I. Blesman, D. A. Polonyankin and V. A. Gorbunov, *Russ. J. Inorg. Chem.*, 2018, **63**, 993; https://doi.org/10.1134/S0036023618080211.
29 A. M. Sofronia, R. Baies, E. M. Anghel, C. A. Marinescu and S. Tanasescu, *Mater. Sci. Eng. C*, 2014, **43**, 153; https://doi.org/10.1016/j.msec.2014.07.023.
30 N. Y. Mostafa, H. M. Hassan and F. H. Mohamed, *J. Alloys Compd.*, 2009, **479**, 692; https://doi.org/10.1016/j.jallcom.2009.01.037.
31 G. Gasquères, C. Bonhomme, J. Maquet, F. Babonneau, S. Hayakawa, T. Kanaya and A. Osaka, *Magn. Reson. Chem.*, 2008, **46**, 342; https://doi.org/10.1002/mrc.2109.
32 V. Putlayev, A. Veresov, M. Pulkin, A. Soin and V. Kuznetsov, *Materialwiss. Werkstofftech.*, 2006, **37**, 416; https://doi.org/10.1002/mawe.200600007.

Received: 24th May 2024; Com. 24/7505